Chapter 5

L-cystine-based Polyurethane as a Drug Delivery Vehicle in Targeted Cancer Treatment and Biomedical Applications

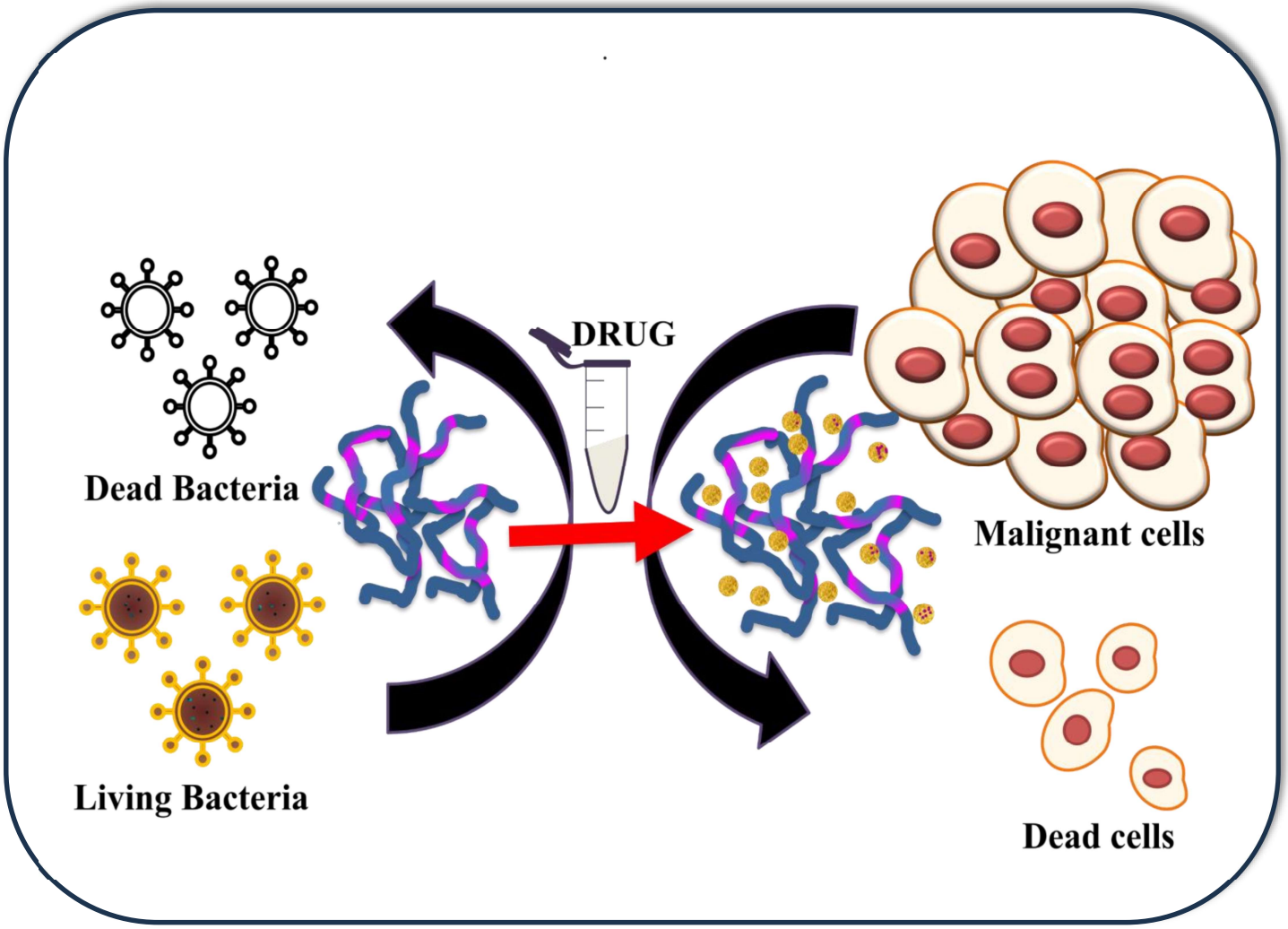

This work has been published in *ACS Applied Bio Materials*.

Chapter 5

5.1 Introduction

Aliphatic PUs have gained attention because of their degradation quality which eliminates the need for surgical removal. The current study introduces a novel class of biodegradable and biocompatible L-Cystine-based aliphatic polyurethanes, paving the way for new L-Cystine-based carriers for drug delivery in cancer therapy and exploiting its antibacterial properties in combination with PU. As chemotherapy suppresses the immune system, cancer patients are more susceptible to bacterial infections. The risk of infections at the site of drug administration or within the body during treatment may be decreased if the drug delivery system includes built-in antibacterial qualities. For instance, it is possible to create biodegradable polymers (PU-CYS) to release antimicrobial compounds that can stop infections or bacterial colonization. Infection at the surgical site is a significant issue when cancer therapy entails surgery (such as tumor removal). By inhibiting bacterial development near the incision or surrounding tissue, an antimicrobial drug delivery vehicle can offer targeted protection, promoting healing and lowering problems. Additionally, the polyurethane's mechanical and thermal response, as well as its drug loading and release performance, were assessed and found to be around 89% release in modified PU (highest) and lowest in PP (control polymer without cystine), i.e., 58% in 48 hours. Cellular studies also confirm the non-toxic behavior of the modified PU and high proliferation due to the incorporation of cystine content.

5.2 Results and Discussion

5.2.1 NMR Spectroscopy

The reaction involved modifying the hydrophilicity and architecture of PU by varying the extent of CYS grafting onto polyurethane. This process involved reacting isocyanate-terminated prepolymer, followed by linking the chain extender (CYS) through amine groups, resulting in a branched structure. Confirmation of the grafting was achieved through ^{1}H and ^{13}C NMR spectroscopy, as depicted in **Figures 5.2a** and **5.2b**, and supported by FTIR and UV-VIS spectroscopy, **Figures 5.2.2a** and **b,** respectively. Coming to the ^{1}H NMR, the disappearance of the peak at 8.71 (due to pure CYS) and the appearance of the peak at 7.96 ppm [176,218] (-NH-, singlet, i) in PU, confirms the reaction between the chain extender with the prepolymer. Again, additional peaks at 4.36 ppm (-CH-, doublet, h) arise from the cystine moiety[101] (^{1}H NMR of pure cystine and PP are given in **Figure 5.2.1 (i) a** and **b,** respectively, as well as the degree of

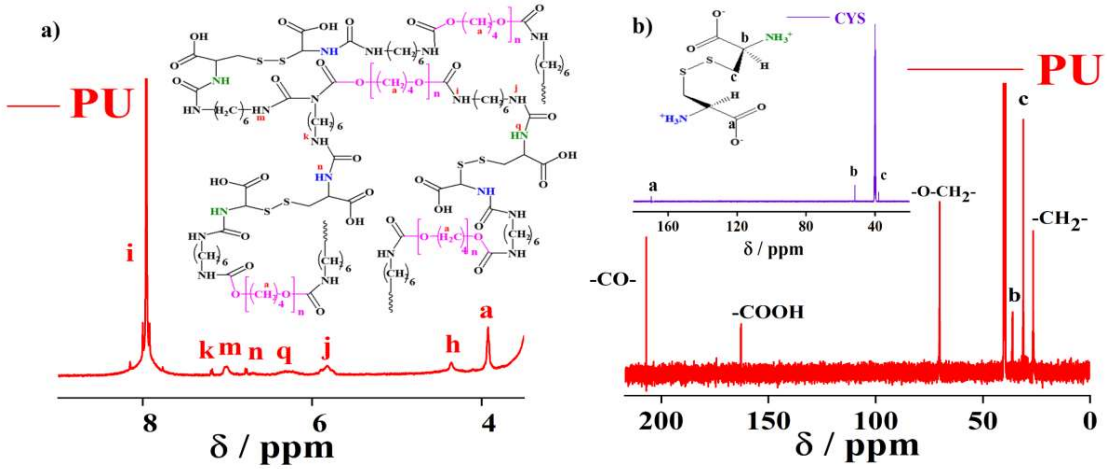

Figure 5.2: a) ^{1}H NMR of PU, the peaks are labeled as "a" and "b" etc.; b**)** ^{13}C NMR spectra of modified PU demonstrate the emergence of new peaks due to polymerization, additional details are provided and labeled as "a" and "b" etc. with the corresponding chemical structure.

polymerization is calculated and found to have 5% tagging). The peak due to -O-CH_2- (PTMG) appears at 3.92 ppm[219] for both the PP and the modified one.

PP has -NH- peak at 7.03 and 5.79[175] the same peak in modified PU shifts to 7.96 and 5.83 ppm, other than this modified one contains four different types of -NH- peaks ranging from (6.25-7.18)[175] ppm. 4

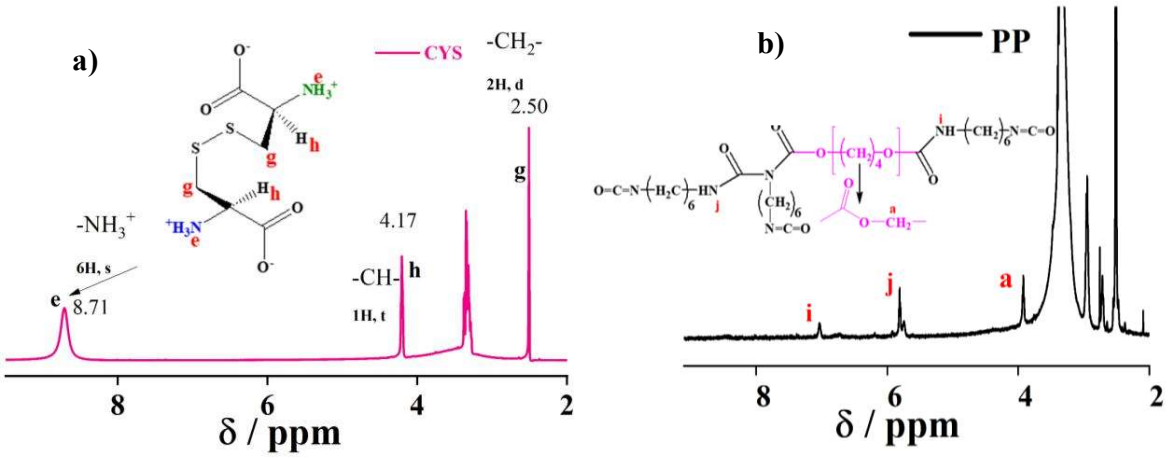

Figure 5.2.1.(i): ^{1}H NMR of a) Pure Cystine and b) Pure Polyurethane (PP)

. ^{13}C spectra of PP display the characteristic peaks at 26.73 ppm (triplet, -CH_2- this unit appears from both PTMG and diisocyanates) and 70.21 ppm {triplet, –CH_2–O, urethane unit}, which shift to 26.61 and 70.09 ppm in PU[220]. The peak for -CO groups in modified PU becomes more prominent and appears at 162 and 206.96 ppm as shown in **Figure 5.2 b** (the ^{13}C NMR for PP is presented in **Figure 5.2.1. (ii)**). It is important to mention that PP is sparingly soluble in DMSO, which might explain the very low intensity of the >CO peak in the ^{13}C spectrum (as well as noise is observed, so it is difficult to distinguish the peak from the noise). An extra peak at around 162 ppm[169] for the -CO group, which comes from cystine's acid group, is absent in PP, confirming the tagging of cystine. However, the same peak for pure cystine appears at 170.11 ppm[221] confirming the zwitterionic form of the original chain extender. The ketone carbonyl resonance cluster, which is located in the 206-ppm range, shows a high-field shift and

intensifies in the spectrum[222,223]. The reason for this enhanced intensity is that the modified polyurethane's (PU) CO group content is larger than that of the pure polyurethane's spectrum.

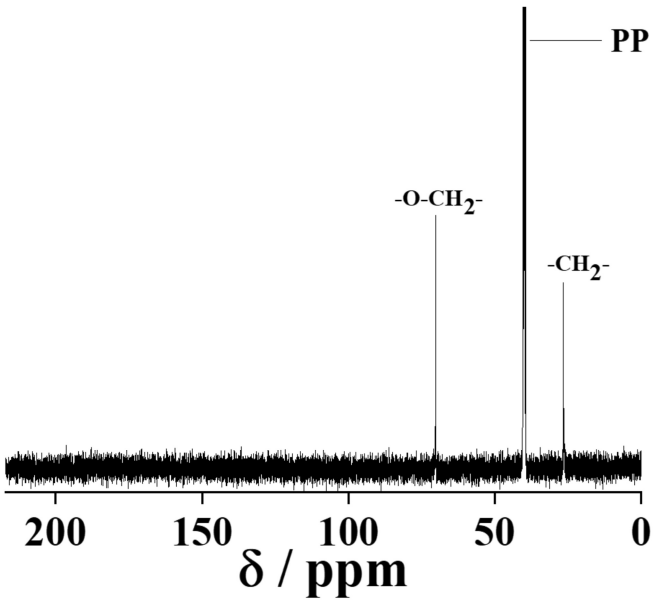

Figure 5.2.1. (ii): ^{13}C NMR of pure polyurethane / PP

5.2.2 Spectroscopic Characterization in Correlation with crystallinity and structural aspect

The FTIR spectral region centered around 3403 cm^{-1} (in modified PU) indicates the >N-H stretching, while the distinct peak of approximately 3331 cm^{-1} in PP suggests a similarity between the two, implying greater intermolecular H-bonding in PU and intramolecular hydrogen bonding in the pure form (PP)[125]. It's worth noting that stronger H-bonding leads to a lower frequency ($\bar{\upsilon}$) shift towards lower values of $\bar{\upsilon}$[224]. Typically, intermolecular hydrogen bonding results in broader bands, whereas bands due to intramolecular H-bonding are sharp and well-defined, as shown in **Figure 5.2.2a**. The FTIR spectral region centered around 3403 cm^{-1} (in modified PU) indicates the >N-H stretching, while the distinct peak of approximately 3331 cm^{-1} in PP suggests a similarity between the two, implying greater intermolecular H-bonding in PU

and intramolecular hydrogen bonding in the pure form (PP)[125]. It's worth noting that stronger H-bonding leads to a lower frequency ($\bar{\upsilon}$) shift towards lower values of $\bar{\upsilon}$[224]. Typically, intermolecular hydrogen bonding results in broader bands, whereas bands due to intra-molecular H-bonding are sharp and well-defined, as shown in **Figure 5.2.2a**.

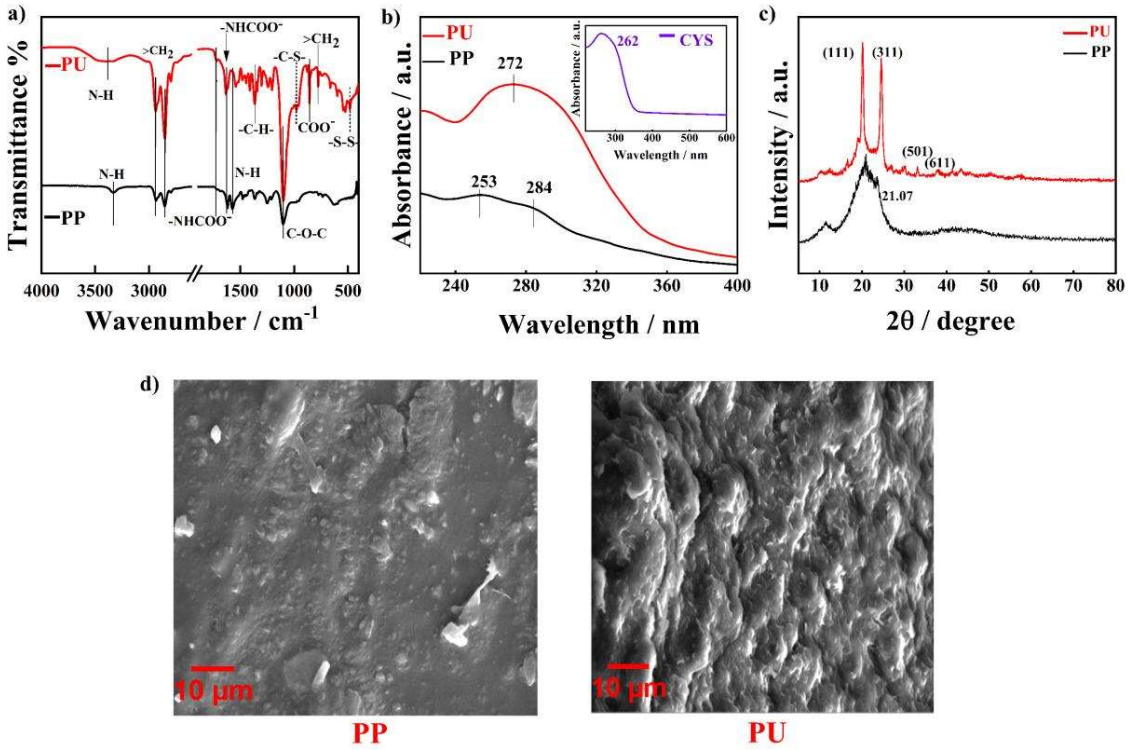

Figure 5.2.2: a) FTIR spectra of all the specimens display shifts in peak positions resulting from interactions; b) UV–VIS spectra illustrate peak positions for the $\pi \rightarrow \pi^*$, $n \rightarrow \pi^*$ transition of the carbonyl peak and marked by vertical lines; c) XRD patterns of all the samples, highlighting their crystalline planes/diffraction angle; and d) SEM images showing the morphology of various PU samples**.**

The evidence supporting the grafting or chemical bonding of polyurethane (PU) onto CYS is evident in the FTIR absorbance peak at 1722 cm^{-1}, attributed to urethane >CO ($-NHCOO^-$)

linkages in both PP and PU[128]. Another>CO peak, due to the H-bonded -NHCOO- group, appears around 1622 cm^{-1} for PP, whereas this peak shifts to 1634 cm^{-1} and intensifies[126] in the PU. A moderately strong peak at 1548 and 1574 cm^{-1} signifies in-plane bending mode of >N-H in both systems, while C-O-C stretching[131] in the hard segment is evident at 1102 cm^{-1}. A weak peak around 978 cm^{-1} is observed for -C-S- in the modified PU, akin to that in CYS (953 cm^{-1})[225]. A strong peak at around 856 and 867 [226] characteristic of CYS, COO^- bond, and the rocking mode of CYS, $-CH_2$, arises near 771 cm^{-1} in PU[227]. The peaks observed at 1388 and 1350 cm^{-1} result from C-H bending of CYS (FTIR of CYS, presented in **Figure 5.2.2. (i)a**), also detected in the modified polymer at 1416 and 1363 cm^{-1}, confirming the presence of CYS integrated with PP[227]. Moreover, the S-S stretching peak of CYS falls within the region of 450-700 cm^{-1} and is evident in the modified PU, confirming the occurrence of polymerization reaction[228].

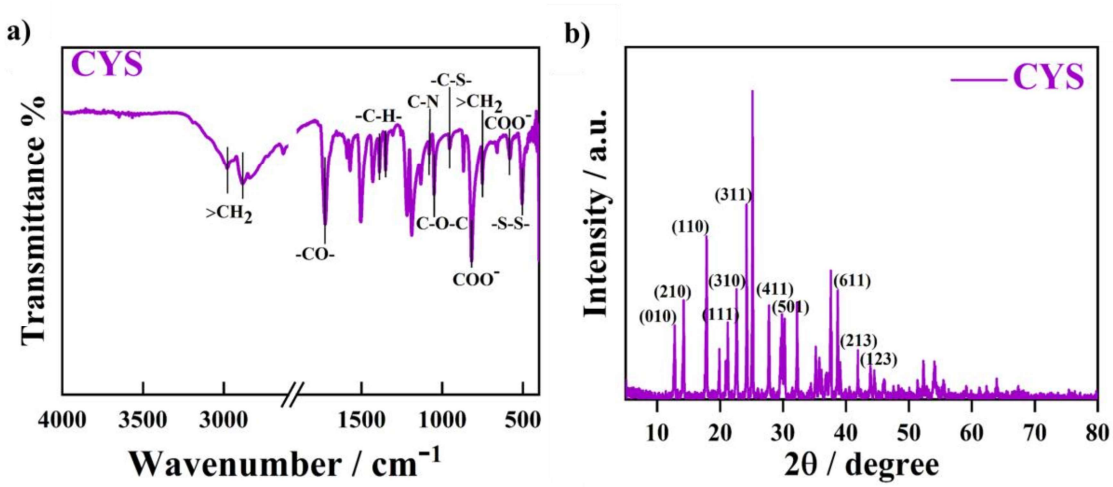

Figure 5.2.2. (i): Pure Cystine a) FTIR, b) XRD.

UV−VIS spectra were examined for all the samples in 200-800 nm range. PP displayed noticeable absorption bands at 253 nm, attributed to π-π* transition[229]. The peak due to n−π*

transition in PP (284 nm) is merged with π-π* in the modified one and becomes broad. Notably, a consistent red shift in the UV−VIS absorption peaks of polymers was observed when moving from PP to modified PU, as shown in **Figure 5.2.2b**. This phenomenon is fairly common in polyurethane, indicating chromophore aggregation in solid state. Thus, adding CYS enhances conjugation, causing the observed redshift[226,230]. X-ray diffraction (XRD) analysis was employed to check the crystallinity of the samples used in this study. PP exhibited a solitary diffuse peak around 2θ ~ 21°, indicating a specific level of crystallinity likely stemming from the crystalline nature of PTMG, which remains distinct within the PU lattice post-polymerization. These results suggest that the soft segment might lack sufficient length for crystallization. However, when CYS is introduced into the PU matrix, it enhances crystallinity, as depicted in **Figure 5.2.2c** (XRD of pure CYS, presented in **Figure 5.2.2. (i)b**). These findings are consistent with prior literature reports[231,232]. To provide a more comprehensive understanding, surface morphology data of all the samples were examined using SEM (**Figure 5.2.2d**), and observed homogeneous blending of the soft and hard segments in both samples[233]. Particularly noteworthy is the well-defined biphasic structure prominently visible in the modified PU image, indicating crystalline zones. Various phases containing different components were observed on the fracture surfaces in this case. With increasing CYS counterparts attached to the system increases, the cross-section of the sheet becomes less uniform, suggesting that the chain extender enhances compatibility with PTMG[140].

5.2.3 Thermal behavior

The modified polymer resembles PP but displays a slight increase in heat of fusion (ΔH) due to the addition of chain extender (CYS). PP exhibits a melting (T_m) endothermic peak at 39

°C due to the soft segment (PTMG), whereas in the modified one (PU), this peak is shifted to 41°C with ΔH values from 33.1 and 45.7 Jg^{-1}, respectively (**Figure 5.2.3a**).

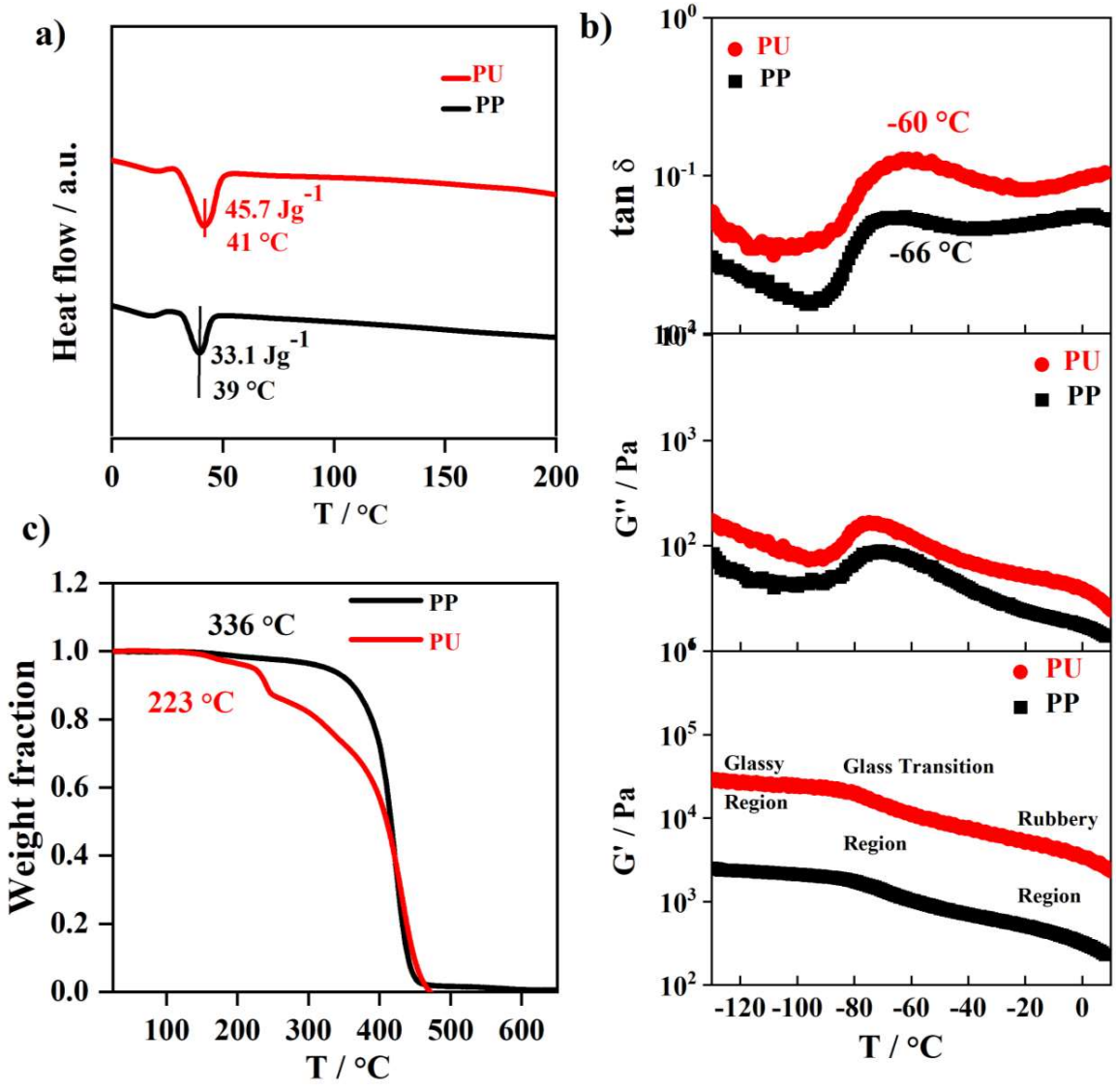

Figure 5.2.3: a) DSC thermograms of various PU samples are displayed, with melting temperatures and heat of fusions indicated in the corresponding color codes; b) represents the storage and loss moduli curves at 1 Hz frequency, loss tangent vs. temperature graph showing the T_g; and c) Thermal stability (TGA thermograms) of all PU samples as measured through a thermogravimetric analyzer.

An important observation is the increase in melting temperature along with an increase in ΔH, which suggests that the addition of hard segments may promote the formation of greater

crystalline zones within the polymer matrix[196]. DMA is an excellent tool for studying the relaxation behavior related to the structure and morphology of the polymers. It allows for the examination of the organization and interactions of hard and soft segments, which significantly influence the physical and mechanical properties of the material. The change in storage modulus (G'), loss modulus(G"), and loss tangent (tan δ) due to temperature provides valuable insights into these properties as shown in **Figure 5.2.3b**. Adding a chain extender with low mass and a long chain diisocyanate (HMDI/hard segment) enhances mobility restrictions, T_g is shifted to higher temperature (-60 ºC for PU from -66 ºC for PP), presumably because of higher crystallinity of PU, and tan δ curve becomes wider in the higher temperature range[234]. Loss factor is the ratio of loss moduli and storage moduli and is found to be higher for PU as compared to PP. Interestingly, the storage modulus of PU is significantly higher than PP (5346 and 539 Pa for PU and PP, respectively, i.e., 891% increase at 20 ºC), mainly arising from the chain extension, in the presence of CYS along with higher crystallinity as observed from DSC and XRD measurements. The loss modulus of PU is also slightly higher than PP, indicating its greater flexibility, and chain extender increases the flexibility[235–237] of the polymer chains by adding segments that can move more freely. Hence, thermal, XRD, and relaxation behavior through DMA are well collaborated and much improved properties of PU are revealed in comparison to prepolymer (PP).

Thermogravimetry (TGA) was used to assess the thermal stability of all the samples. Thermal degradation under an inert atmosphere was determined by identifying the temperature, which 5% weight loss was noticed for the sample. No major degradation has been observed below 150°C temperature in all the PU samples (**Figure 5.2.3c**). The degradation temperatures are found to be 223 and 336 °C for PU and PP, respectively, showing lower degradation of CYS-

modified PU. The PP shows two-step degradation arising from hard and soft segment degradation, while PU exhibits three-step degradation, and extra initial weight loss is due to breakage of the S-S bond present in CYS (DTG graph shown in **Figure 5.2.3. (i)**)[238]. The addition of a hard segment increases the crystallinity while lowering the thermal stability of the urethane linkage in PU[239].

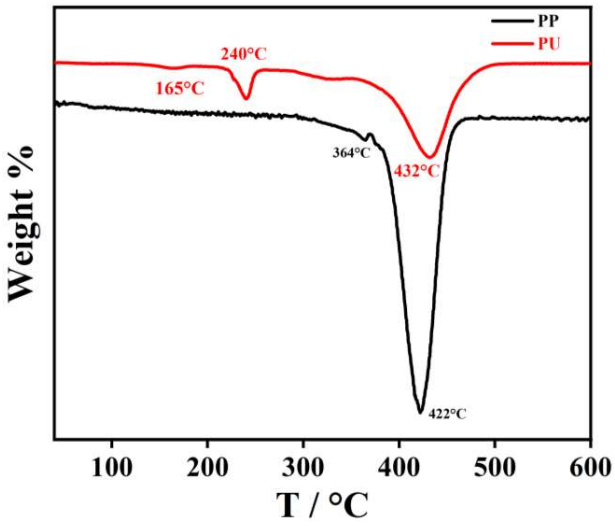

Figure 5.2.3.(i): DTG graph of both the polymers.

5.2.4 Sustained reléase of drug using varying PU structure

The cumulative release of paclitaxel from both PP and PU in PBS solution over time has been shown in **Fig. 5.2.4a**. A similar amount of drug (5 wt.% with respect to polymer weight) was embedded in both PP and PU. PP releases 58% of the embedded drug in 48 h while PU releases 89% in the same time. Observing the release pattern of paclitaxel in PBS buffer over time reveals a steady and sustained release from all the systems, likely due to stronger H-bonding interactions between drug and polymer as confirmed through UV-VIS data shown in **Fig. 5.2.4 b** and **c**, and the respective values are reported in **Table 5.2.4.1.** PP shows the absorption peak at 253 nm, which has shifted to 283 nm in drug-embedded PP, while PU

exhibits a major absorption peak at 272 nm, which has shifted to 294 nm in drug-embedded PU. A significant redshift for both cases indicates strong interaction between the respective

Table 5.2.4.1 shows the difference in UV-Vis wavelength

UV-VIS	Sample (Wavelength) / nm	Sample + Drug (Wavelength) / nm	Difference
PP	253	283	30
PU	272	294	22

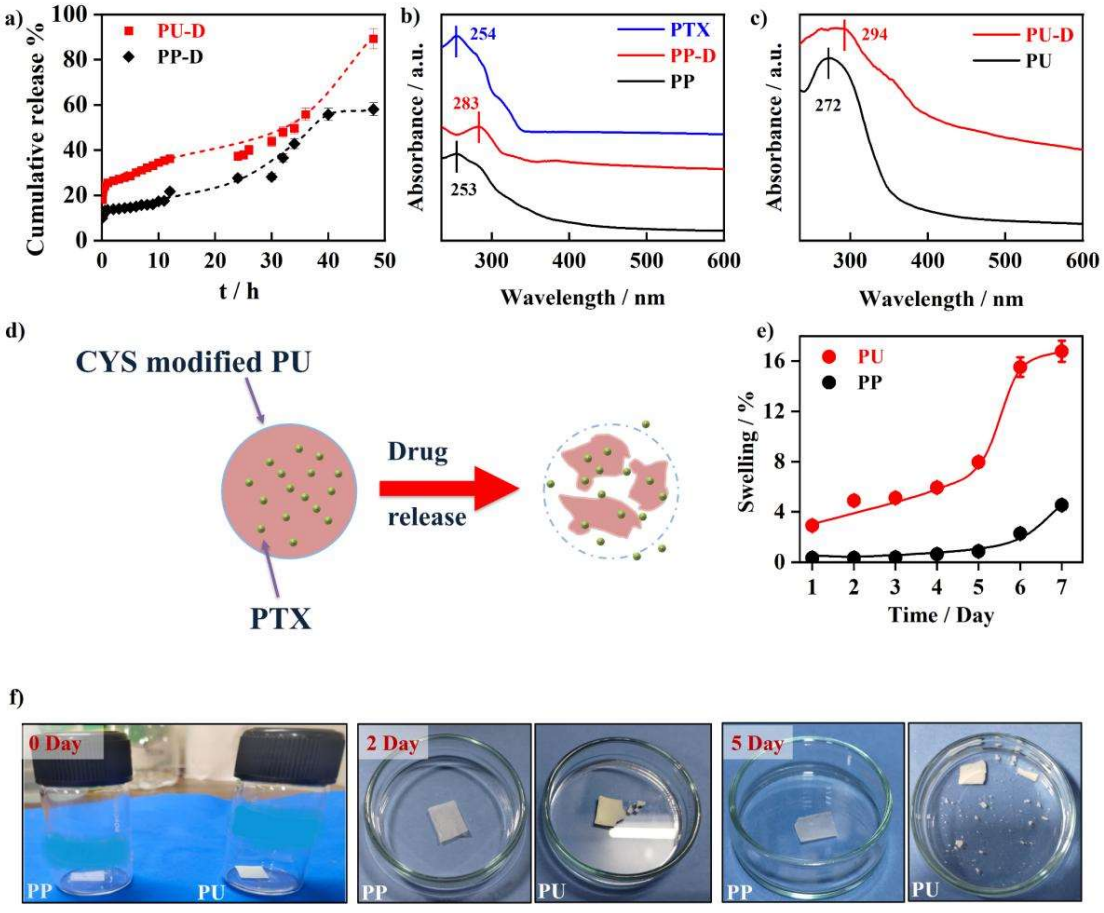

Figure 5.2.4: a) Cumulative drug release from the specimens demonstrates a sustained release profile from the polymers; b) & c) UV-VIS spectra of the indicated samples revealing polymer-drug interactions, with vertical lines marking the respective peak positions/shifts resulting from hydrogen bonding interactions; d) Schematic of drug release from the polymer matrix; e) Swelling as a function of time showing the hydrophilic/hydrophobic nature of both the polymers; and f) Degradation images of both PP and PU films up to 5 days in PBS media.

polymers that trigger sustained release of PTX from the matrix polymer. Kinetic parameters using the Higuchi models show $r^2 \sim 0.97$ and 0.93 for PP and PU, respectively, indicating a non-Fickian release mode (**Figure 5.2.4. (i)** represents the mechanism of drug release using various kinetic models, and corresponding values are reported in **Table 5.2.4.2**).

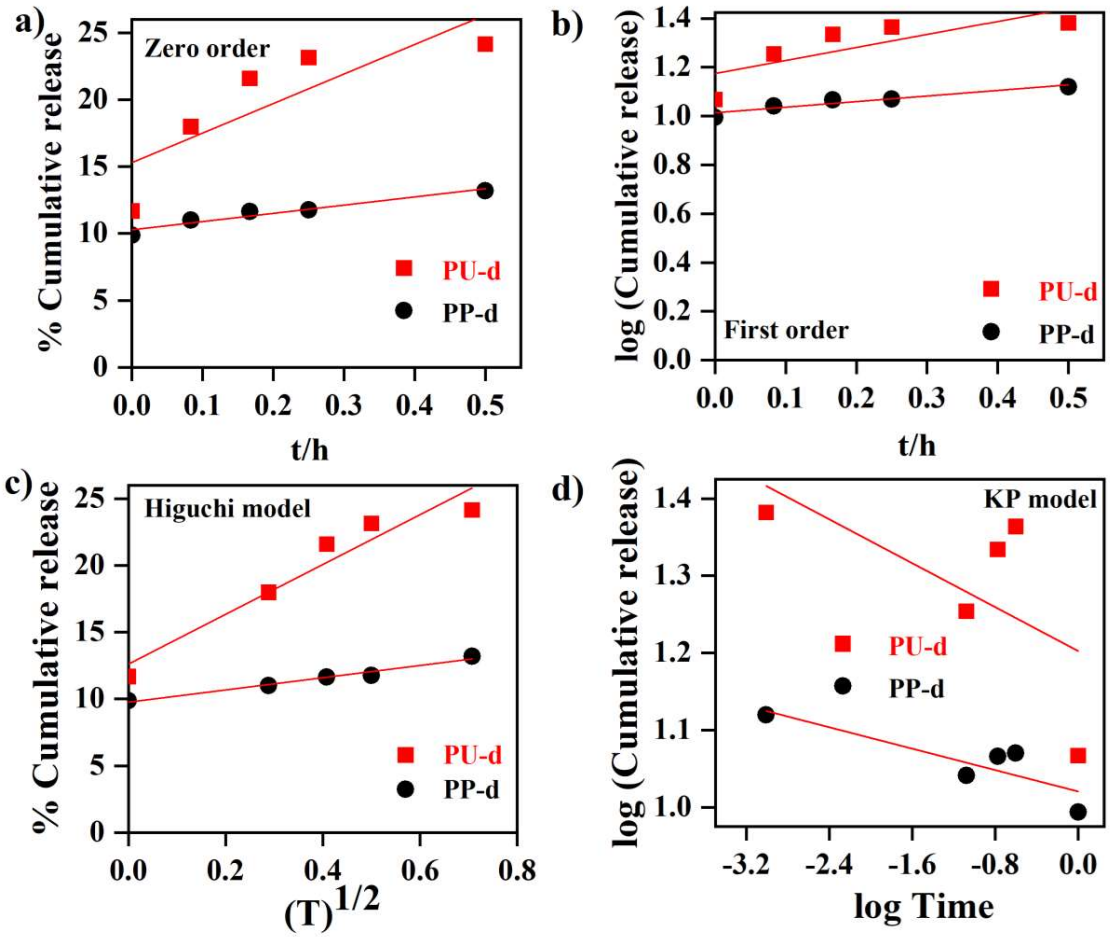

Figure 5.2.4. (i): represents the mechanism of drug release using various kinetic models

The drug-polymer interaction is shown via FTIR as well in **Figure 5.2.4. (ii)** In modified PU, we see a broad peak at 3403 cm^{-1} (intermolecular) where spectra of -NH and -OH are

merged, but in the drug-loaded PU, the distinct peaks of H-bonded -NH (at 3329) and -OH at 3476 cm^{-1} are observed. Now, in pure polymer initially it has an intramolecular peak at 3331 cm^{-1}, but after drug loading, we see two peaks at 3347 (H-bonded -NH) and 3477 cm^{-1} (H-bonded -OH). This fact also supports the larger H-bonded interaction of the drug with both moieties.

Table 5.2.4.2 represents the corresponding values of kinetics

Compositions	Zero Order	First Order	Higuchi Model	KP Model
PP-d	Slope =6.1±0.9 Intercept=10.3±0.2 r^2=0.93	Slope =0.2±0.04 Intercept=1.01±0.01 r^2=0.91	Slope =4.6±0.4 Intercept=9.8±0.2 r^2=0.97	Slope =-0.03±0.01 Intercept=1.02±0. 01 r^2=0.74
PU-d	Slope =22.1±8.4 Intercept=15.3±2.2 r^2=0.70	Slope =0.5±0.2 Intercept=1.17±0.06 r^2=0.63	Slope =18.6±2.9 Intercept=12.60±1.3 r^2=0.93	Slope =-0.07±0.05 Intercept=1.2±0.07 r^2=0.39

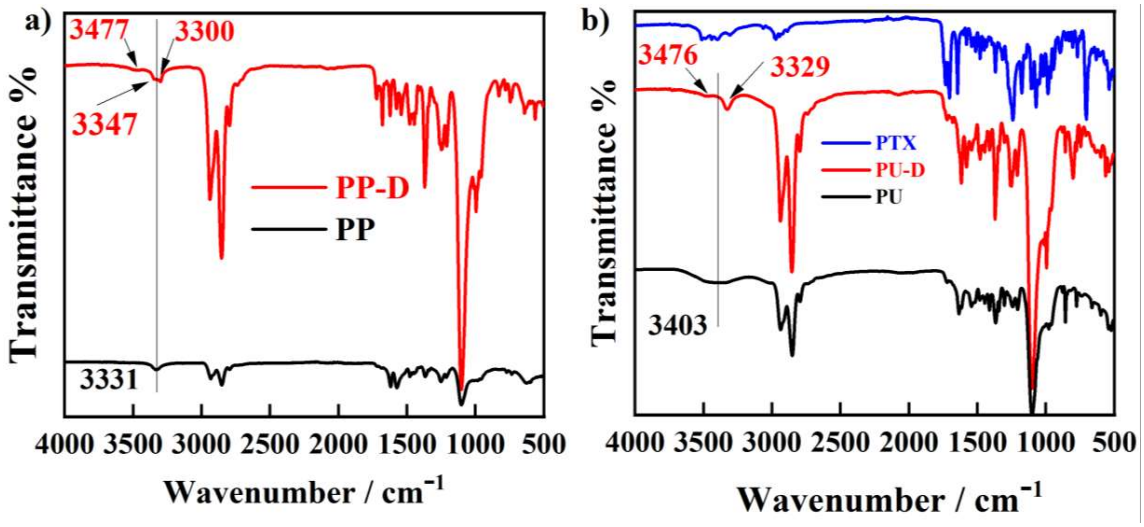

Figure 5.2.4. (ii): FTIR analysis to check drug-polymer interaction, in a) PP, H-bonding interaction is intramolecular before and after (3331 to 3300 and 3347 cm^{-1}) drug loading, b)

for PU, the H-bonding, which is initially broad (3403 cm^{-1}), becomes sharp after drug attachment.

Again, the interaction between PP and PTX alone is probably going to be weaker and dominated by basic hydrophobic interactions or van der Waals forces. By creating new interactions (such as H-bonds and disulfide interactions), the cystine alteration in CYS-PU can change the chemical nature, potentially resulting in a more advantageous situation from interaction point of view. The drug's affinity for the PU-CYS matrix is enhanced by the hydroxyl groups (or other polar groups) found in PTX.

Water seeps into the polymer matrix, dissolving the drug therein. It then facilitates the drug's migration to the surface, breaching the boundary layer and allowing the drug to reach the media. PP is hydrophobic, whereas incorporating a hydrophilic counterpart (CYS) increases its hydrophilicity and makes the drug accessible for media dissolution. Hydrophilic chain extenders attract water molecules when the polyurethane matrix comes into contact with bodily fluids**.** Increased hydrophilicity of PU as compared to PP has been shown through swelling studies in **Figure 5.2.4e**. As the polymer matrix swells, its structure becomes more porous. This increased porosity facilitates the diffusion of the drug molecules out of the matrix. The absorbed water molecules create water channels inside the polymer network, these channels provide pathways for the drug molecules to move out of the matrix, and mobility increases[240,241]. The sudden increase in drug release of PU after 40 hours occurs as the moiety starts to degrade with time in the release media, leading to rupture into small fragments[242,243] as shown through photographic images during swelling studies (**Figure 5.2.4f**). The nature of drug release from the hydrophilic CYS-based PU has been depicted in **Figure 5.2.4d**. However, cystine-based polyurethane exhibits steady and sustained release and is explained well by the strong interaction and greater

swelling of the hydrophilic PU, incorporated through the chemical bonding (chain extension) of CYS in PP to make a bigger PU. Remarkably, in previously reported results[244] in the absence of GSH (Glutathione), PTX was shown to be released from the PU micelles in an inefficient and delayed manner, with about 5% released in the first 4 hours and about 11% released in the next 48 hours. On the other hand, due to the instability of polyurethane micelles, the release of PTX was markedly accelerated in the same buffer solution containing 10 mM GSH, with 26% released in 4 hours and nearly 60% released in 48 hours. But with our system, which uses CYS-modified PU, we don't require GSH to accelerate the release, and we have 89% release in 48 hours. Here, hydrophilicity dominates overall and promotes the release at a higher rate for the PU-CYS system.

5.2.5 Biocompatibility and *in-vitro* treatment efficacy

Ensuring biocompatibility in drug carriers is fundamental for their successful integration and application in biomedical fields, ultimately enhancing the safety, efficacy, and reliability of therapeutic interventions for patients. Biocompatibility was estimated via cell adhesion by capturing phase-contrast images of 3T3 and SiHA cells cultured with the material, demonstrating enhanced cell adhesion on the polymer structure as seen by the well-spread morphology (**Fig. 5.2.5a and b** for 3T3 and SiHA, respectively). The images of the 3T3 cell line were taken at 20x where whereas SiHA images were taken at 40x resolution to get a clearer cell morphology, since 3T3 has a length of (50-100) µm, whereas SiHA has a length of (20-50) µm. However, sometimes the length varies depending on the material bed we are using. The OD values are 101% for 3T3 and 149% for SiHA cells, after 24 hours[245,246] of cellular assessment, data confirm better adherence of material (PU) on cancer cells compared to healthy muscle cells (**Fig. 5.2.5c and d**). Much higher OD in the case of the PU-SiHA

system indicates the greater efficacy of CYS-based PU for better cancer treatment. The greater adhesion on cancer cells could potentially enhance targeted delivery of anticancer drugs. This specificity might reduce off-target effects and increase the concentration of therapeutic agents at the tumor site, improving treatment efficacy[215,247]. Enhanced Permeability and Retention (EPR)[214,248] effect is indeed observed in cancer cells. This phenomenon is primarily associated with the distinct features of tumor vasculature and the microenvironment of solid tumors. Tumors often have abnormal and highly permeable blood vessels due to rapid and disorganized angiogenesis[249].

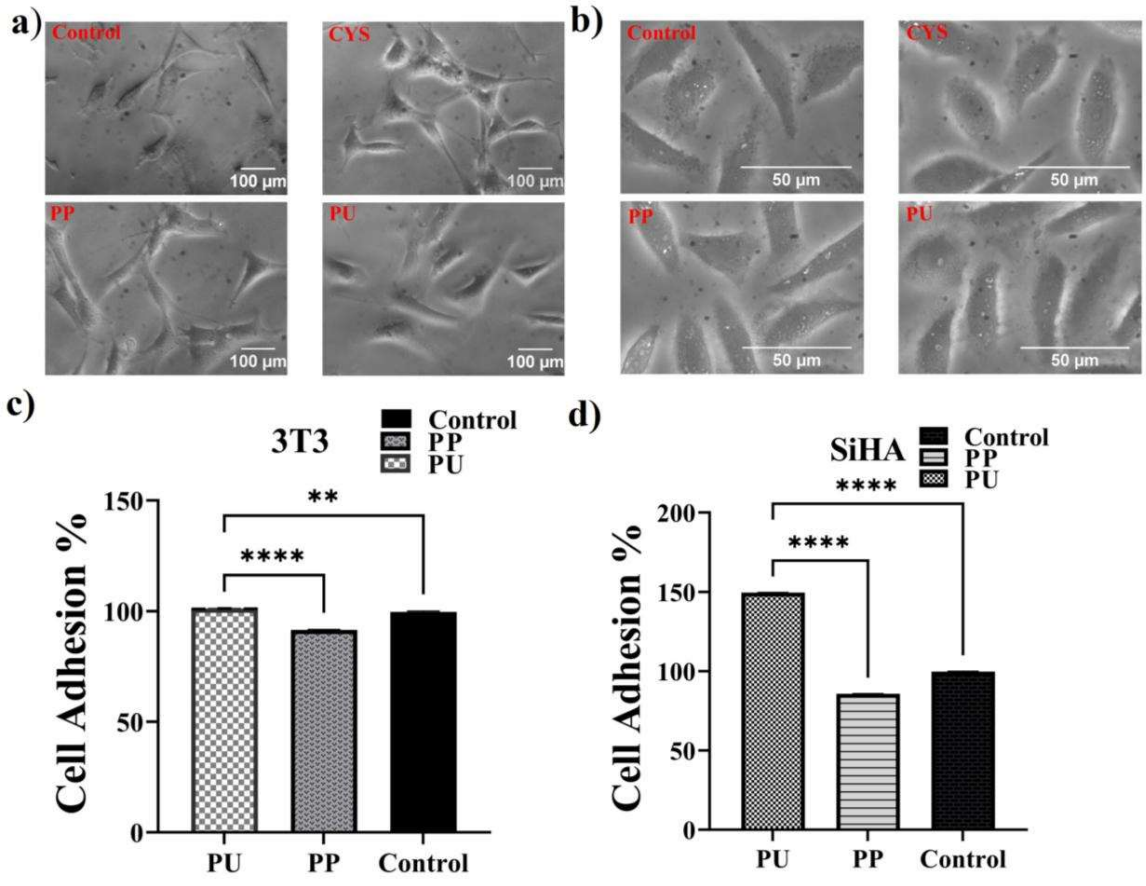

Figure 5.2.5: Biological responses of all the polymers assessed through cellular studies, a) Morphology of 3T3 cells grown on PP and PU surfaces as captured through microscopy on a gray filter after 1 day of sample proliferation (cell adhesion magnification: 20×); b) Morphology

of SiHA cells grown on PP and PU surfaces as captured using microscope on a gray filter after 1 day of sample proliferation (cell adhesion magnification: 40×); c) Evaluation of cell adhesion using optical density profile data for adhered 3T3 cells across the sample bed; and d) Evaluation of cell adhesion using optical density profile data for adhered SiHA cells across the sample bed.

This leads gaps between endothelial cells, enabling macromolecules penetrate more easily than normal tissues. Thus, the carrier's EPR effect is predominantly evident in *in-vitro* experiments, in cancer cells as well. Hence, the current *in-vitro* study has only validated the drug delivery capabilities of the newly designed L-CYS-based polyurethane, serving as a proof-of-concept. Moreover, *in-vitro* studies are necessary to determine the dissimilarities in cell-killing effectiveness between free PTX and drug-loaded polymers. Furthermore, biological responses of all the samples (pure PP and PU) are evaluated through MTT assay on 3T3 and SiHA cell lines for three consecutive days, from varying the concentration of 20 to 100 µg/ml, revealing that modified PU exhibits superior biocompatibility over PP and the corresponding OD value and AOPI images for 20 µg/ml are present in the **(Figure 5.2.5.1 a, c** for 3T3 and **d, f** for SiHA) which is at per the literature reports.[101] The PU shows more than 90% cell viability even in higher concentration (100 µg/ml), after the 3rd day of study in both cell lines **(Figure 5.2.5.1 b** for 3T3 and **e** for SiHA). Modified PU shows 104% cell viability (at 20 µg/ml) and maintains 91% cell viability even at 100 µg/ml after a three-day study on 3T3 cells, in contrast to SiHA cells, where the viability is increased from 144% to 163% by increasing the concentration from 20 to 100 µg/ml. In both cell lines, viability for PP decreases with time in 3T3; the viability is 90% after the concentration goes to 100 µg/ml, but in SiHA, at this concentration, the cell viability drops to 70%. So this signifies the obsession of CYS-modified PU for cancer. Thereby, the addition of CYS moiety to the PU system enhances its biocompatibility as well as bioavailability to tumor cells and makes it one of the most effective carriers for drug delivery in practical applications.

Pure drug trends to show increased cell viability (reduced cell mortality) over time, although slightly higher cell killing was observed on day 1 (**Figure 5.2.5.2a** for SiHA cell line and the corresponding AOPI image for 20 µg/ml shown in **Figure 5.2.5.2 b**) due to immediate

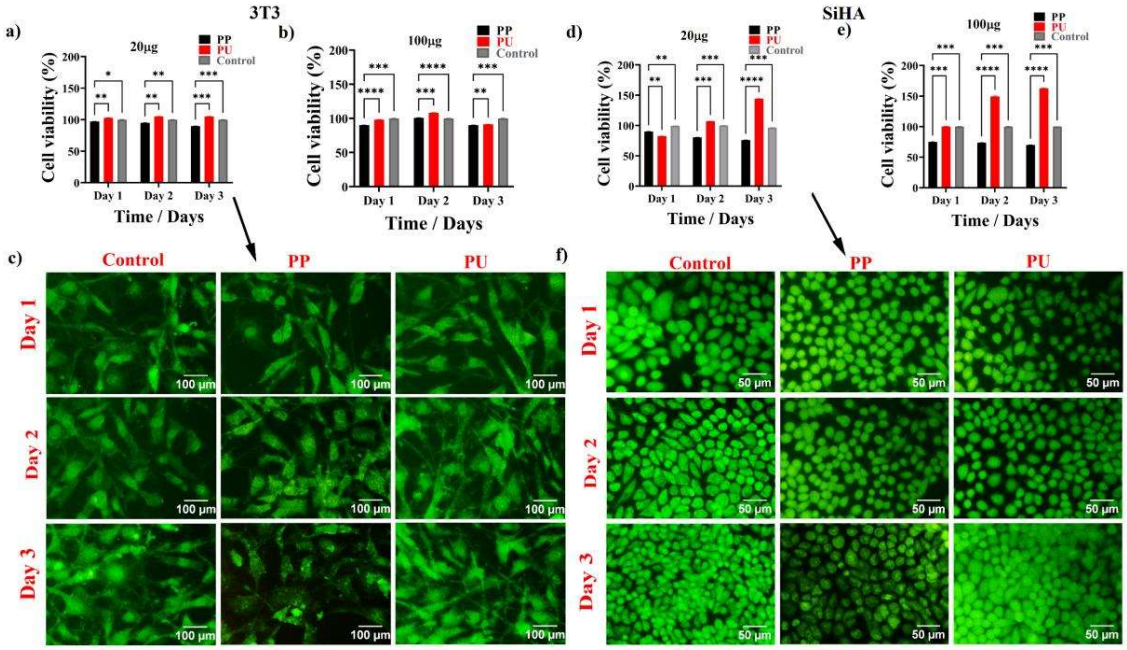

Figure 5.2.5.1: a and b show cell viability for the 3T3 cell line at 20 µg/ml and 100 µg/ml concentration, whereas d and e show cell viability for the SiHA cell line at 20 µg/ml and 100 µg/ml concentration, respectively. The corresponding AOPI images for 3T3 and SiHA cells at 20 µg/ml are Figures 5.2.4 (i) c and f, respectively.

exposure to the cellular media. For the 3T3 cell line[250], there is an increase in cell death with time (**Figure 5.2.5.2c** for the 3T3 cell line, and the corresponding AOPI image at 20 µg/ml in **Figure 5.2.5.2d**).

Cancer and normal cells have a similar share of target molecules (enzymes or receptors), resulting in normal cells being inadvertently affected. Here comes into play the vehicle

modified PU (20 µg/ml) which selectively kills 59% of SiHA cells after a consecutive study of three days, whereas the same drug-loaded system maintains 85% of 3T3 cells viable at the same dosage and when the dose increased to 100 µg/ml it keeps up to 76% 3T3 cells alive (**Figure 5.2.5.3 a** for SiHA and **b** for 3T3 cells). Their cellular behavior changes due to hypoxia (low oxygen level) or acidic surface, which is why they engulf extracellular fluids (Endocytosis), nutrients, and building blocks (Cystine is an alpha amino acid or building unit of protein), under stressed conditions to meet their heightened metabolic rate. Cancer cells adapt several mechanisms to uptake larger molecules to sustain their rapid growth and survival in the harsh tumor environment.

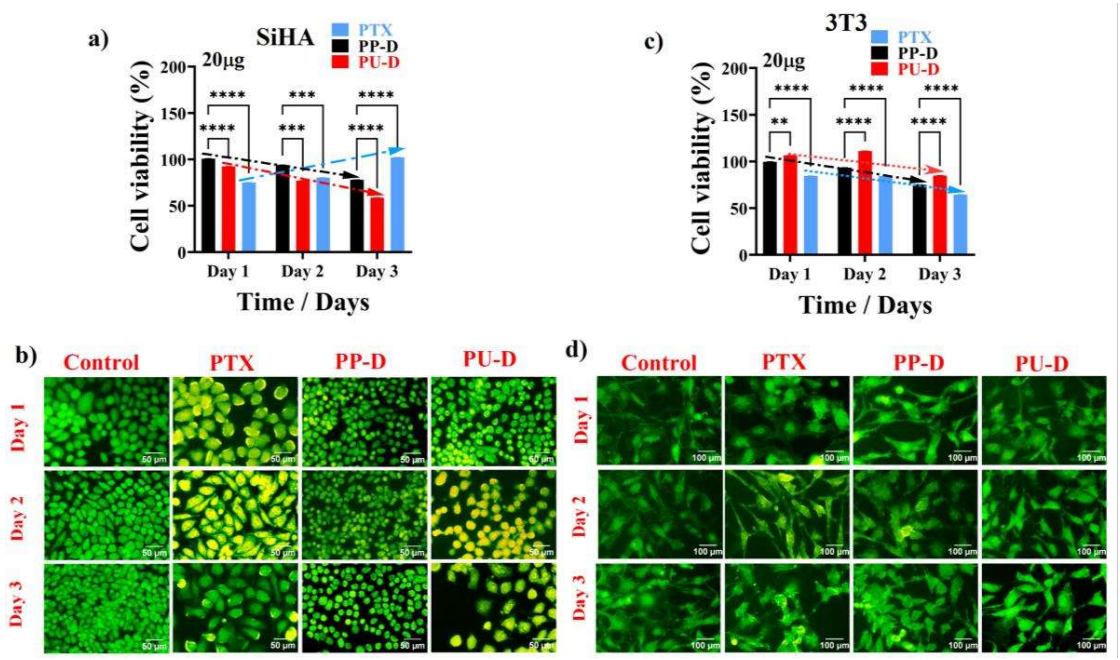

Figure 5.2.5.2: a) *In vitro* cytotoxicity of pure drug and, drug-loaded PUs on SiHA cells at various time intervals assessed using the MTT assay at a concentration of 20 µg/ml, b) Fluorescence images of SiHA cells after AO/EB staining, treated with pure drug and drug-loaded polymers at a concentration of 20 µg/ml, captured at 20× magnification, c) *In vitro* cytotoxicity of pure drug and drug-loaded PUs on 3T3 cells at different time intervals evaluated using the MTT assay at a concentration of 20 µg/ml; and d) fluorescence images of 3T3 cells after AO/EB staining, treated with pure drug and drug-loaded polymers at a concentration of 20 µg/ml, captured at 20× magnification.

Whereas normal cells and cancer cells have different cell surface characteristics and extracellular matrix (ECM) environments, pure polyurethane tends to adhere to normal cells better. The extracellular matrix (ECM) of normal cells is generally more stable and homogeneous, making it easier for polyurethane to stick to it. On the other hand, cancer cells frequently display changed ECM composition and cell surface characteristics, which can weaken polyurethane adherence. This understanding can be used for developing advanced cancer therapies.

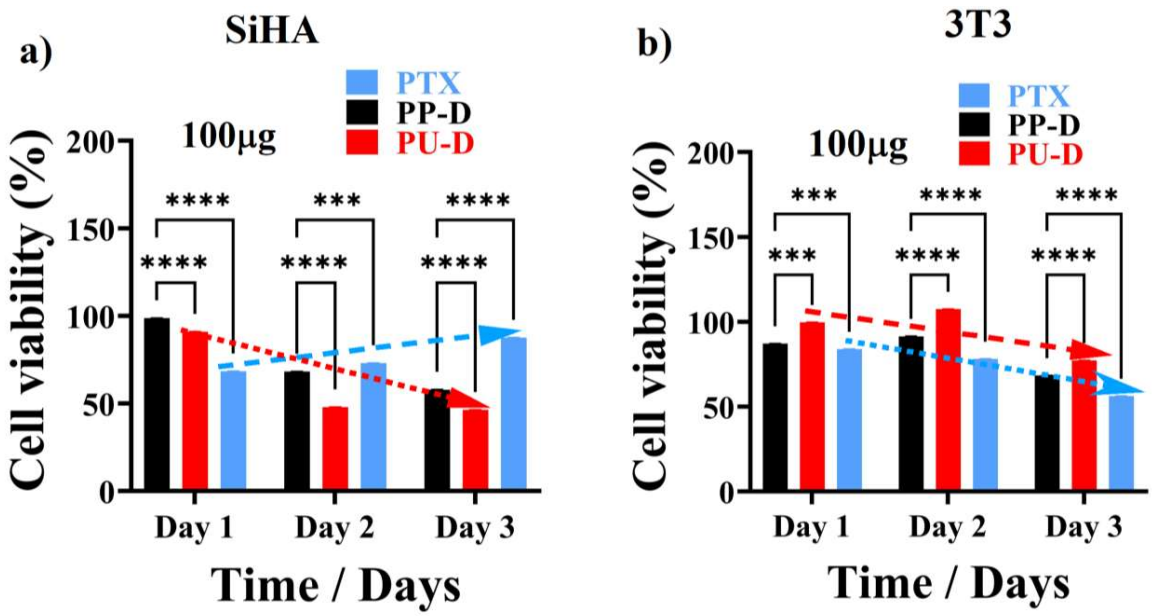

Figure 5.2.5.3: MTT assay data for biocompatibility of all the drug-loaded samples at 100 µg/ml concentration, a) SiHA and b) 3T3

To comprehend the mechanism of cell killing or drug-induced apoptosis by drug-loaded vehicles or pure drugs, both cell types were examined using fluorescent imaging after staining with acridine orange (AO) and propidium iodide (PI). This dual staining technique differentiates between normal and apoptotic cells by assessing membrane permeability. AO can penetrate the cell membrane, bind to DNA, and emit green fluorescence, while PI emits red fluorescence.

Typically, dead cells, which allow both AO and PI to enter, appear red. In contrast, healthy cells, which only allow AO, appear green. Cells that exhibit an orange-yellow shade after AO/PI staining indicate apoptosis or early necrosis, with red fluorescence signifying compromised membrane integrity, while normal healthy cells show green fluorescence. Drug-loaded PU-treated SiHA cell line shows a reduced cell density and predominantly apoptotic nature, while 3T3 cells remained viable on day 3, consistent with the MTT assay results. However, tumor cell killing efficiency is highest for PTX-embedded PU while its normal cell killing rate is lowest which proves to be its greater efficacy for targeted tumor treatment as compared to pure drug or drug-embedded prepolymer (PP) which in turn indicates the greater efficiency of CYS as the chain extender to design a proficient drug delivery vehicle.

5.2.6 Antibacterial Assay

5.2.6.1 Determination of MIC

The antibacterial activity against two control bacterial strains was assessed, with the results presented in **Table 5.2.6.** Cystine usually exhibits highly efficient inhibitory effects on Gram-positive and Gram-negative bacteria, with a MIC range of 2 mg/ml and 1 mg/ml, respectively (the corresponding graph for Cystine's anti-bacterial property/MIC is presented in **Figure 5.2.6.1a** and **b** for *E. coli* and *S. aureus,* respectively).

Table 5.2.6: MIC for Cystine and its corresponding polymer (PU) against two bacterial strains:

Microorganisms	**MIC (mg/ml)**	
	Cystine	**PU**
S. aureus	2	20
E. coli	1	Not effective for *E. coli*

Cystine is created through the oxidation of two cysteine molecules, which creates a disulfide (−S−S−) bond. This disulfide bond can interact with thiol groups (−SH) in bacterial proteins,

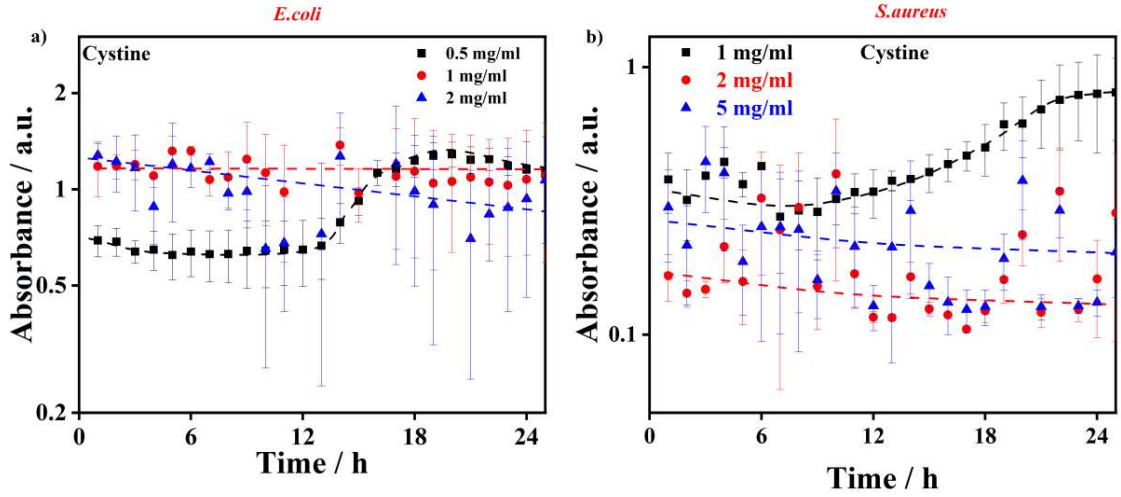

Figure 5.2.6.1: shows the minimum inhibitory concentration (MIC) of pure cystine moiety in a) *E.coli* from concentrations ranging (0.5 to 2) mg/ml and b) *S. aureus* from concentrations ranging (1 to 5) mg/ml.

disrupting bacterial cell functions. Additionally, it can chelate essential nutrients or interfere with their uptake by bacterial cells[251–253]. By binding to critical nutrients or competing with bacterial transport systems, cystine effectively starves bacteria of necessary resources, inhibiting their growth and proliferation.

Similarly, the antibacterial effect of both samples has been shown in **Figure 5.2.6** (**a** for pure polymer and **b** for PU in *E. coli,* whereas **c** for pure polymer and **d** for PU in S. aureus, respectively) for both bacterial strains.

Pure polyurethane does not inhibit bacterial growth up to 40 mg/ml for both bacterial strains, while cystine-modified PU restricts the growth of *S. aureus* only at 20 mg/ml. However, it does not restrict the growth of *E. coli* even at 50 mg/ml. Gram-positive bacteria (*S. aureus*) have a

thick peptidoglycan layer in their cell walls, while Gram-negative bacteria (*E. coli*) have a thinner peptidoglycan layer[254,] but they possess an outer membrane that serves as an additional barrier. This outer membrane[255] can protect them from various antibacterial agents, making them more resistant. The cystine-modified PU may target the cell wall components of *S. aureus*[256]

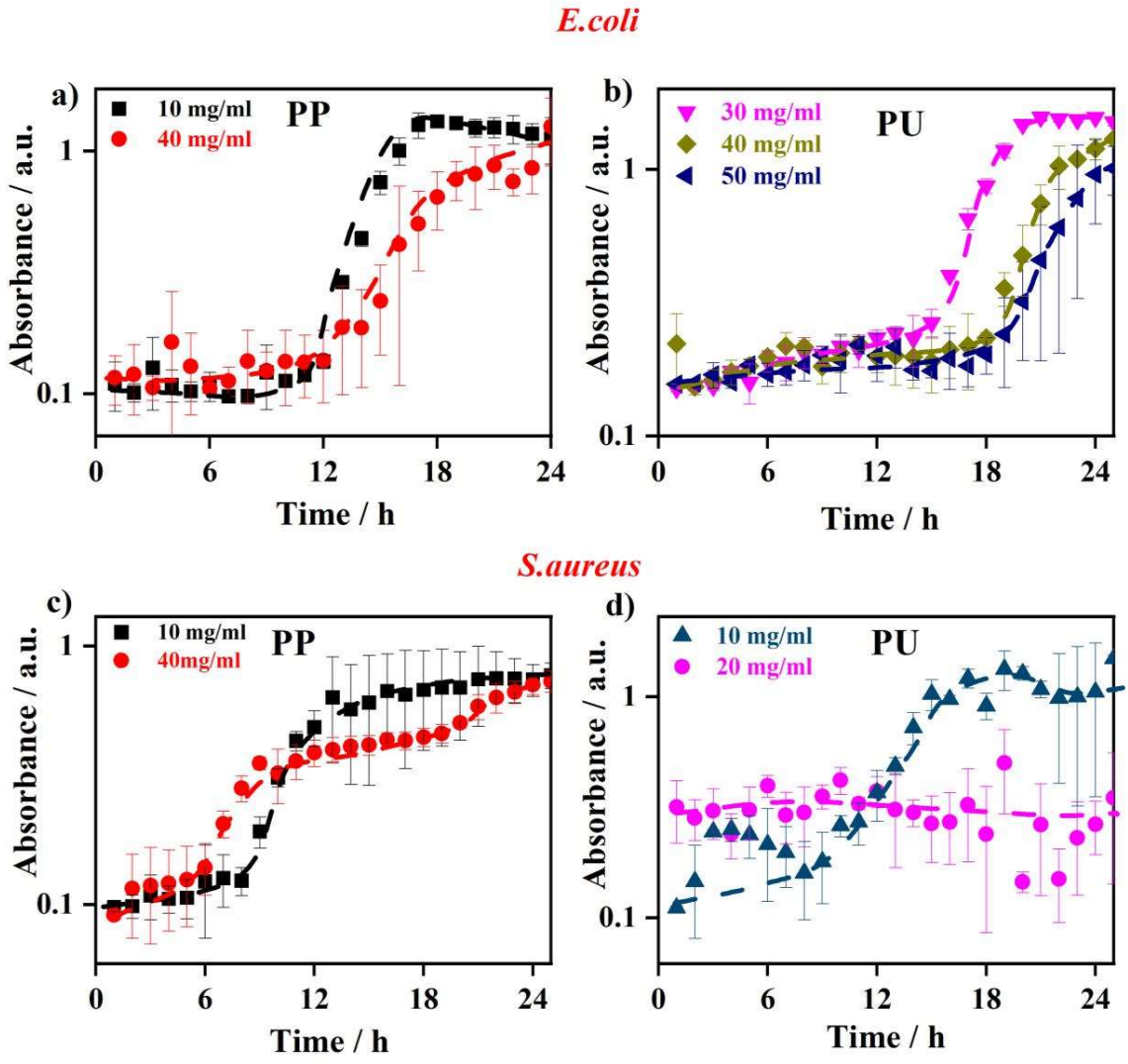

Figure 5.2.6: represents the antibacterial assay for both samples in two different bacterial strains, in *E. coli* for a) PP; b) cystine-modified PU, and in *S. aureus* for c) PP; and d) cystine-modified PU.

hence, it might not work as effectively against *E. coli* due to their protective outer membrane. In addition to the outer membrane, *E. coli* is often more prone to forming biofilms on surfaces like polyurethane. Biofilms are highly resistant to antibacterial treatments, which further reduces the material's effectiveness. Again, CYS-modified PU may have the potential to upset their efflux processes by interfering with the membrane integrity or by directly suppressing efflux pump activity. As a result, antibiotic sensitivity may rise. This is worth mentioning that due to the low tagging percentage of cystine (~5%) on the polymer backbone, the antibacterial activity of the cystine-modified PU is lower compared to pure CYS.

5.2.6.2 ROS Assay

The ROS assay utilized *S. aureus* and *E. coli* (as shown in the corresponding **Figure 5.2.6.2**), to check if bacterial growth is inhibited by ROS mechanism. The behavior of cystine about ROS activity can vary depending on its context and interactions with other materials, such as polyurethane. Cystine, through its disulfide (−S−S−) bond, can contribute to oxidative stress by generating reactive oxygen species when it interacts with cellular components. This can happen through redox cycling, where cystine is reduced to cysteine and then creates ROS as by-products. In biological systems, an imbalance may tip this balance, leading to oxidative stress and increased ROS activity. Grafting of Cystine onto the PU backbone modulated its interaction with the environment. The PU matrix might enhance the antioxidant properties (synergistic effect) of cystine by providing a stable environment where the thiol groups of cysteine (formed from cystine) can efficiently scavenge ROS. This could result in an overall neutralization of ROS, making it suitable for applications where oxidative stress is a concern. The bacteria treated with modified PU (PU-CYS) exhibit notably reduced fluorescence intensity in comparison to the untreated controls, suggesting that the material is effective in mitigating oxidative stress.

Given that GSH may aid in neutralizing ROS, the decrease in ROS may result from increased amounts of GSH being maintained[257]. In this study, the PU material demonstrated a more controlled and effective pathway for significant reduction of ROS in both Gram-positive and Gram-negative bacteria[258,259]. The polymer might be affecting membrane-associated enzymes responsible for ROS generation, such as NADPH oxidases or other redox enzymes anchored in

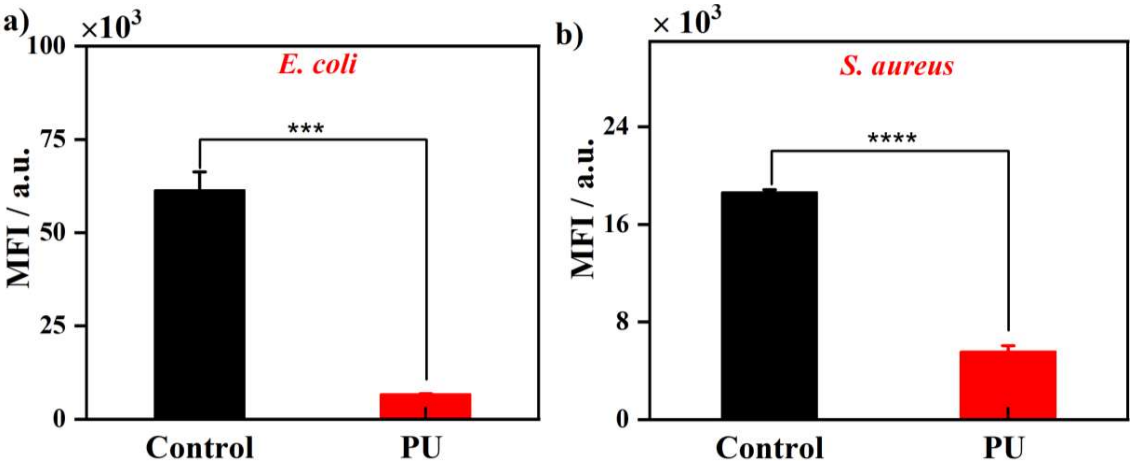

Figure 5.2.6.2: represents the ROS assay for modified PU samples, in the presence of two different bacterial strains, gram-negative **a)** *E. coli* and gram-positive **b)** *S. aureus* ($p<0.05$).

the outer membrane or periplasmic space. Without crossing the membrane, the polymer could still modulate its function by inhibiting or interacting with these enzymes on the cell surface or modifying the local redox environment near the outer membrane. So, ROS may not be the major reason for inhibiting the growth of *S. aureus*. In summary, while reduced ROS levels might affect both Gram-positive and Gram-negative bacteria, the selective killing of Gram-positive bacteria by CYS-modified PU most likely involves a combination of factors related to cell wall interactions, the specific properties of the polyurethane material, and due to the presence of CYS moiety. Antioxidants are viable therapeutic agents that can be used effectively against specific infections; this application of antioxidants (CYS-modified PU) against diseases is the first of its kind and indicates its novelty towards disease cure, including tumor treatment through steady

and sustained drug release.

5.3 Conclusion

L-cystine (dimer) based polyurethane has been synthesized using HMDI and PTMG as the hard and soft segments, to generate biodegradable polymer (PUs) with advantageous biocompatibility and bioavailability qualities. NMR, FTIR, and UV studies confirmed the addition of cystine to PU chains (as a chain extender), having no adverse effect on SiHA (tumor cells) and 3T3 (normal muscle cells). In comparison to pure polyurethane, CYS-modified PU has enhanced porosity, hydrophilicity, and degradation behavior, which increased the drug (PTX) release up to 89% in comparison to prepolymer (PP), having only 58% in a similar time frame (48 hours). Cellular assessment confirms the improved adherence of material (PU) to cancer cells, and the OD values for 3T3 and SiHA cells are 101% and 149%, respectively, indicating the tumor treatment in a targeted manner. Modified PU selectively kills 59% of SiHA cells while the same drug-loaded system retains 85% of 3T3 cells viable at the same dosage. Importantly, the release from the carrier is sustained and controlled, specifically targeting the cancer cell for three days, which reduces the need for regular drug administration. In addition, the CYS-modified PU shows antibacterial properties against *S. aureus* with an MIC of 20 mg/ml. Cystine's antibacterial property adds to PU and reduces ROS of the system, where oxidative stress is concerned, and effectively inhibits the growth of *S. aureus*. CYS-modified PU shows protracted drug release, high biocompatibility, along with antibacterial properties, which makes it a suitable candidate to be used as an anti-cancer targeted drug delivery system.